

Mitochondrial regulation of GPX4 inhibition-mediated ferroptosis in acute myeloid leukemia

Hiroki Akiyama

The University of Texas MD Anderson Cancer Center <https://orcid.org/0000-0003-2627-1055>

Ran Zhao

UTMDACC <https://orcid.org/0000-0003-3390-5343>

Lauren Ostermann

MD Anderson Cancer Center <https://orcid.org/0000-0002-3330-2174>

Ziyi Li

MD Anderson Cancer Center

Natalia Baran

The University of Texas MD Anderson Cancer Center <https://orcid.org/0000-0003-0618-4798>

Samar Yazdani

The University of Texas MD Anderson Cancer Center

Edward Ayoub

The University of Texas MD Anderson Cancer Center <https://orcid.org/0000-0003-1321-0114>

Malcolm Pryor

The University of Texas MD Anderson Cancer Center

Yuki Nishida

MD Anderson Cancer Center

Po Mak

The University of Texas M.D. Anderson Cancer Center

Vivian Ruvolo

The University of Texas MD Anderson Cancer Center <https://orcid.org/0000-0003-4363-7258>

Bing Carter

The University of Texas M.D. Anderson Cancer Center

Michael Andreeff

The University of Texas MD Anderson Cancer Center <https://orcid.org/0000-0002-1144-1958>

Jo Ishizawa (✉ jishizawa@mdanderson.org)


The University of Texas MD Anderson Cancer Center <https://orcid.org/0000-0001-8566-7370>

Article

Keywords:

Posted Date: March 14th, 2023

DOI: <https://doi.org/10.21203/rs.3.rs-2657913/v1>

License:  This work is licensed under a Creative Commons Attribution 4.0 International License.
[Read Full License](#)

Additional Declarations: **Yes** there is potential conflict of interest.

Version of Record: A version of this preprint was published at Leukemia on December 26th, 2023. See the published version at <https://doi.org/10.1038/s41375-023-02117-2>.

Abstract

Resistance to apoptosis in acute myeloid leukemia (AML) cells causes refractory or relapsed disease, associated with dismal clinical outcomes. Ferroptosis, a mode of non-apoptotic cell death triggered by iron-dependent lipid peroxidation, has been investigated as potential therapeutic modality against therapy-resistant cancers, but our knowledge of its role in AML is limited. We investigated ferroptosis in AML cells and identified its mitochondrial regulation as a therapeutic vulnerability. GPX4 inhibition induces ferroptosis in AML cells, accompanied with characteristic mitochondrial lipid peroxidation, exerting anti-AML effects in vitro and in vivo. Electron transport chains (ETC) are primary sources of coenzyme Q10 (CoQ) recycling for its function of anti-lipid peroxidation in mitochondria. We found that the mitochondria-specific CoQ potently inhibited GPX4 inhibition-mediated ferroptosis, suggesting that mitochondrial lipid redox regulates ferroptosis in AML cells. Consistently, Rho0 cells, which lack functional ETC, were more sensitive to GPX4 inhibition-mediated mitochondrial lipid peroxidation and ferroptosis than control cells. Furthermore, degradation of ETC through hyperactivation of a mitochondrial protease, caseinolytic protease P (ClpP), synergistically enhanced the anti-AML effects of GPX4 inhibition. Collectively, our findings indicate that in AML cells, GPX4 inhibition induces ferroptosis, which is regulated by mitochondrial lipid redox and ETC.

Introduction

Acute myeloid leukemia (AML) is the most common acute leukemia in adults. Despite recent progress in molecularly targeted therapies, the 5-year overall survival rate is only about 30% [1]. This is mainly due to frequent relapse or refractory disease, which carries a dismal prognosis; these patients' one-year survival rate is only 10% [2]. As a major cause of such therapy resistance, AML cells develop resistance to apoptosis induction through numerous mechanisms [3, 4], underlining the unmet need for the development of alternative therapeutic strategies that overcome apoptosis resistance.

Pathways of non-apoptotic regulated cell death are of growing interest in cancer research. One such form of regulated cell death is ferroptosis, which is characterized by iron dependency and triggered by the accumulation of lipid peroxidation on cellular membranes [5]. Increasing evidence from solid tumor studies supports the therapeutic potential of ferroptosis induction through its distinct mechanism of cell death independent of apoptosis. Major defense mechanisms against ferroptosis include the system x_c^- /glutathione/glutathione peroxidase 4 (GPX4) pathway [6, 7] and GPX4-independent pathways that utilize endogenous radical-trapping antioxidants such as coenzyme Q₁₀ (CoQ) [8-11] or tetrahydrobiopterin [12, 13]. Among them, GPX4 is the only enzyme that can directly reduce lipid peroxides and its inhibition results in ferroptosis. GPX4 is a selenoprotein, whose translation is regulated by a unique protein synthesis mechanism that requires selenium. However, because of its high rank in selenoprotein synthesis hierarchy, the expression of GPX4 is relatively retained even under selenium deficiency [14] suggesting its importance of cellular homeostasis.

AML cells exhibit increased reactive oxygen species production [15] and active iron uptake [16], both known determinants of ferroptosis susceptibility. We therefore hypothesize ferroptosis as a vulnerability in AML. While ferroptosis has been investigated recently in AML [17-21], the molecular mechanisms of GPX4 inhibition in AML remain largely unknown.

In the present study, we sought to elucidate the molecular mechanisms of GPX4 inhibition–induced ferroptosis in AML. We identified mitochondrial involvement in ferroptosis in AML cells, which provides a molecular rationale for targeting this disease-specific vulnerability to enhance the anti-leukemia effects of GPX4 inhibition.

Results

GPX4 is a potential therapeutic target in AML and has possible prognostic relevance

To evaluate the therapeutic potential of targeting ferroptosis-regulating genes including *GPX4* in a variety of cancer cell lines, we analyzed Cancer Dependency Map (DepMap) datasets using shinyDepMap [22], a tool that combines CRISPR and shRNA screening data of 423 cancer cell lines. This tool enabled us to predict the essentiality of genes of interest across cancer cell lines as well as the selectivity of the gene essentiality among distinct cell types. In particular, we investigated ferroptosis suppressor genes annotated on FerrDb, a manually curated database of ferroptosis regulators and their disease associations [23] [24] (FerrDb V2, last access; 8/13/2022). *GPX4* was the second-ranked gene with the high essentiality among the top 10 ferroptosis suppressors (efficacy score; $X = -1.21$), following *MTOR* as the top ($X = -1.454$) (**Fig. 1A**). In addition, the selectivity of *GPX4* (selectivity score; $Y = 0.799$) was much higher than that of *MTOR* ($Y = 0.076$), indicating that the essentiality of *GPX4* is more cell line–specific. Importantly, when the cell lines were grouped by tumor type, AML was among those that are highly dependent on *GPX4* (**Fig. 1B**). Of note, consistently, *MTOR* exhibits high dependency not only in AML but more prominently in other tumor types (Fig. S1A). These analyses suggest that targeting GPX4 may have specific roles in AML.

We next evaluated the potential impact of *GPX4* on the survival of AML patients, utilizing a dataset from The Cancer Genome Atlas (TCGA), and found that high *GPX4* expression was associated with shorter patient survival (**Fig. 1C** and Fig. S1B–D). A multivariate Cox proportional hazard model adjusted for age, gender, and cytogenetic risk groups also revealed a significant association between higher GPX4 expression and shorter survival (**Fig. 1D**). These results are consistent with previous reports [25] [26] and suggest GPX4 as a novel prognostic factor in AML patients.

GPX4 inhibition induces ferroptosis in AML cells *in vitro* and *in vivo*

To test the anti-leukemia effects of the pharmacological inhibition of GPX4, we utilized ML210 [27, 28], to date a well-established, proteome-wide specific inhibitor of GPX4. Protein expression levels of GPX4 were determined and found variable among 11 AML cell lines (**Fig. 2A**). Next, we determined GPX4 inhibition–induced cell death as the percentage of cells positive for annexin V and/or DAPI to capture both apoptotic

and non-apoptotic cell death including ferroptosis. In OCI-AML3 cells, ML210 increased both, annexin V-positive and DAPI-positive fractions, which were effectively suppressed by the lipophilic antioxidants liproxstatin-1 (Lip1) and α -tocopherol (α Toc) as well as the iron chelator deferoxamine (DFO) (**Fig. 2B**). These data indicate that, although annexin V is usually used as a marker of apoptosis, annexin V-positive AML cells that result from GPX4 inhibition are ferroptotic. This is consistent with previous findings demonstrating that lipid peroxidation upon ferroptosis can cause phosphatidylserine externalization without caspase activation [29]. Consequently, the pan-caspase inhibitor z-VAD-FMK did not inhibit ML210-induced cell death (**Fig. 2C** and Fig. S2A, B). Lip1, α Toc, and DFO consistently suppressed ML210-induced lipid peroxidation, which was detected with C11-BODIPY (**Fig. 2D**). The iron-dependent lipid peroxidation and cell death induced by ML210 were confirmed in MOLM-13 and OCI-AML2 cells as well (Fig. S2C-F).

Next, we evaluated the efficacy of ML210 across 11 AML cell lines. Sub-micromolar concentrations of ML210 induced cell death in most cell lines (**Fig. 2E**). Pearson correlation analysis revealed a negative correlation between ML210 sensitivity and GPX4 protein expression level (**Fig. 2F**), which suggests that GPX4 expression levels are potential predictors of AML cell sensitivity to GPX4 inhibition. To further assess the effects of endogenous GPX4 level on ferroptosis, we supplemented cell culture media with selenium to enhance GPX4 biosynthesis. Supplementing culture media with seleno-L-methionine (SLM) increased GPX4 expression levels in OCI-AML3 and MOLM-13 cells (Fig. S2G). We further generated Doxycycline (Dox)-inducible short hairpin RNA (shRNA) constructs to knockdown eukaryotic elongation factor, selenocysteine-tRNA specific (*EEFSEC*), which is required for selenoprotein translation [30]. The Dox-induced knockdown of *EEFSEC* abrogated SLM-induced GPX4 upregulation (Fig. S2H), confirming that GPX4 upregulation occurs through increased protein synthesis of GPX4. As expected, AML cells cultured in SLM-supplemented media are resistant to ML210 (Fig. S2I).

We also assessed ML210 sensitivity in *TP53*-mutant AML cell lines, which served as an *in vitro* model of one of the most clinically challenging genetic subtypes of AML. ML210 exerted its anti-leukemia effects independently of *TP53* mutational status, as it had similar efficacy among isogenic MOLM-13 cells with *TP53* deletion or hotspot mutations (**Fig. 2G**). The knockdown of mutant *TP53* in Kasumi-1 cells harboring the *TP53*^{R248H} mutation did not alter sensitivity to ML210 (**Fig. 2H**). Taken together, ML210 exerts anti-leukemia effects independently of *TP53* mutation status.

We then treated primary cells derived from AML patients (n = 13) or healthy bone marrow donors (n = 12) with ML210. AML patients included those who relapsed after or developed resistance to multiple regimens and/or those with *TP53* mutations (Table S1). Most of the primary AML samples tested were sensitive to ML210 (**Fig. 2I** and S2J). Three samples showed resistance to ML210, but we could not identify any common features explaining the resistance, including prior regimens, cytogenetics, or mutations. Independently, cell death induced in primary cells from healthy bone marrow donors (HD) was significantly lower than that induced in patient samples.

We next introduced Dox-inducible shRNAs targeting *GPX4* (shGPX4) into OCI-AML3 cells (OCI-AML3-shGPX4-1 or -2 cells) (**Fig. 3A**). Treatment with Dox for 96 hours resulted in lipid peroxidation, followed by cell death induction at 120 hours (**Fig. 3B, C** and Fig. S3A), demonstrating that GPX4 downregulation induces lipid peroxidation prior to the cell death. The findings were confirmed in MOLM-13 cells and OCI-AML2 cells transfected with the same shRNAs (**Fig. 3D, E** and Fig. S3B, C). In addition, *GPX4* knockdown sensitized OCI-AML3-shGPX4-1 and -2 cells to ML210 at a dose that were not effective by itself (**Fig. 3F**), consistent with the aforementioned negative correlation between GPX4 protein expression and sensitivity to GPX4 inhibition.

To determine the anti-leukemia effect of GPX4 inhibition *in vivo*, we labeled OCI-AML3-shGPX4-2 cells with luciferase and transplanted them into NSG mice. After engraftment was confirmed by bioluminescent imaging (BLI) (Fig. S3D), the mice were given regular water (vehicle) or tetracycline water to knockdown *GPX4* in leukemia cells. Tetracycline treatment significantly prolonged mouse survival (median survival 74 days vs 55 days), confirming that GPX4 inhibition exerts anti-leukemia effects *in vivo* (**Fig. 3G**).

Cell death induced by *GPX4* knockdown was abrogated by Lip1 and aToc but not by DFO (Fig. S3E-F), likely because of the low concentration of DFO used in these assays. The maximal tolerable dose of DFO in AML cell lines (4 μ M for OCI-AML3 cells) (Fig. S3G) was much lower than those used in previous studies of ferroptosis in cancers other than leukemia (up to 100 μ M) [6, 31]. Thus, the inherent anti-leukemia effects of DFO present a limitation in determining the protective effects of iron chelation against GPX4 inhibition-induced ferroptosis in AML cells. In fact, Lip1 completely blocked cell death induced by a high concentration (>20 times the EC50) of ML210, whereas DFO did not (Fig. S3H), suggesting that low-dose DFO blocks ferroptosis less efficiently than Lip1 does. Indeed, lipid peroxidation in OCI-AML3-shGPX4 cells (**Fig. 3B**, Fig. S3A) was more potent than that induced by ML210 in OCI-AML3 cells (**Fig. 2D**). Therefore, we speculate that the degree of ferroptosis induced by GPX4 inhibition in our genetic knockdown models was greater than that which could be rescued by low-dose DFO.

Mitochondrial lipid peroxidation and electron transport chain complexes regulate AML cell ferroptosis

Because mitochondria are the centers of cellular redox and iron metabolism, we next investigated the involvement of mitochondria in AML cell ferroptosis. Morphologically, evaluation by transmission electron microscopy showed that, compared with control cells, ML210-treated OCI-AML3 cells had smaller mitochondria with an electron-dense mitochondrial matrix (**Fig. 4A**). This is consistent with previous ferroptosis studies in non-leukemia models [6, 32]. ML210-treated OCI-AML3 cells also had disorganized cristae with “vesicular” morphology, a phenomenon similar to the finding reported to occur during apoptosis induction in HeLa cells [33]. Functionally, ML210 increased mitochondrial superoxide production, which was largely blocked by Lip1, aToc, and DFO, in AML cells (**Fig. 4B, C**, Fig. S4A, B). This suggests that the mitochondrial superoxide induced by GPX4 inhibition is mostly iron-dependent lipid peroxidation. Indeed, flow cytometry with MitoPerOx staining, which specifically detects lipid peroxidation in mitochondria, revealed that ML210 consistently increased mitochondrial lipid peroxidation (**Fig. 4D**).

Dox-induced *GPX4* knockdown also increased mitochondrial superoxide production and lipid peroxidation in OCI-AML3 cells (**Fig. 4E** and Fig. S4C) and MOLM-13 cells (Fig. S4D).

A previous study using mouse embryonic fibroblasts (MEFs) demonstrated that the mitochondria-targeting antioxidant mitoquinone mesylate (MitoQ) is far less potent than the non-targeting antioxidant decylubiquinone (DecylQ) in protecting cells from GPX4 inhibition–induced ferroptosis [34]. This suggests that ferroptosis usually arises from a redox imbalance in cytoplasm but not in mitochondria. We confirmed that the concentration of MitoQ required to block ML210-induced cell death was more than 5-fold that of DecylQ in MEFs (**Fig. 4F**). In contrast, and unexpectedly, MitoQ was as potent as DecylQ in blocking ferroptosis in OCI-AML3 cells treated with ML210 (**Fig. 4G**), suggesting that AML cell ferroptosis is regulated predominantly by mitochondrial, rather than cytoplasmic, lipid peroxidation. In addition to MitoQ, MitoTEMPO, another mitochondria-targeted antioxidant, also blocked cell death caused by ML210 treatment or by Dox-induced *GPX4* knockdown, further supporting the mitochondrial regulation of ferroptosis in AML cells (**Fig. 4H, I** and Fig. S4E, F).

Next, to investigate the role of mitochondrial respiration, the center of mitochondrial redox metabolism, in AML cell ferroptosis, we utilized HL-60-Rho0 cells, which were established by chronically exposing HL-60 cells to ethidium bromide to specifically deplete mitochondrial DNA and thus render them deficient of mitochondrial respiration [35]. Immunoblot analysis revealed that Rho0 cells had non-detectable levels of electron transport chain (ETC) complex proteins (subunits in complexes I, II, III, and IV) but unchanged levels of GPX4 expression (**Fig. 4J**). Both mitochondrial DNA–encoded proteins (UQCRC2 and MTCO1) and nuclear DNA–encoded proteins (SDHB and NDUFB8) were depleted in Rho0 cells, which indicates that the loss of mitochondrial DNA–encoded ETC subunits results in defects across the complexes. This is supported by a recent report of proteome-wide analysis of 143B-Rho0 cells [36]. Notably, HL-60-Rho0 cells are nearly 10 times as sensitive to ML210 as their wild type (WT) controls (HL-60-RhoWT) (**Fig. 5K**). This was unexpected because the original report that defined ferroptosis showed that the sensitivity of Rho0 cells was similar to that of control cells in 143B cells [6]. Furthermore, prominent mitochondrial lipid peroxidation was induced in Rho0 cells by almost 10-fold lower concentration of ML210 when compared to RhoWT cells, confirming that Rho0 cells are more sensitive to GPX4 inhibition–induced mitochondrial lipid peroxidation in the AML cell line (**Fig. 5L**). These data suggest that the intact protein expressions of ETC complex proteins protects AML cells from GPX4 inhibition–mediated ferroptosis, perhaps uniquely in AML cells.

GPX4 inhibition–mediated ferroptosis is synergistically enhanced by hyperactivation of mitochondrial caseinolytic protease P

Given Rho0 AML cells' higher ferroptosis sensitivity, we investigated the therapeutic potential of a combination of ferroptosis induction and ETC downregulation in AML. We previously demonstrated that the hyperactivation of the mitochondrial protease caseinolytic protease P (ClpP) by imipridones (ONC201 or ONC212) induces the degradation of multiple ETC subunits to disrupt mitochondrial respiration and exerts cancer-selective lethality [37]. Indeed, the combination of ML210 and ONC201 induced synergistic

cell death in OCI-AML2 and MOLM-13 cells (**Fig. 5A**). The combinatorial anti-leukemia effect was associated with the cumulative induction of lipid peroxidation and mitochondrial superoxide production (**Fig. 5B, C**). Synergistic cell death was also observed for the majority of primary AML cells tested, as determined by combination indexes (**Fig. 5D**). Importantly, primary cells from healthy bone marrow donors exhibit significantly less cell death upon the combinatorial treatment compared to AML cells (**Fig. 5E**, and Fig. S5A).

Furthermore, synergistic cell death was induced when the genetic activation of ClpP using a Dox-inducible *CLPP-Y118A* hyperactivated mutant was combined with ML210 and when Dox-inducible *GPX4* knockdown was combined with ONC201 and ONC212 (**Fig. 5F–H**, Fig. S5B, C). Supporting these findings, our re-analysis of a previously published CRISPR screening data of NALM6 leukemia cells treated with imipridones [38] revealed *GPX4* to be one of the top hits; knockdown of *GPX4* sensitized cells to ClpP hyperactivation (**Fig. 5I**). In addition to *GPX4*, genes essential for selenoprotein synthesis (*SEPSECS*, *EEFSEC*, *PSTK*, *SEPHS2*) [39] were also top hits, suggesting that the inhibition of GPX4's function as a selenoprotein is important for the synthetic lethality of GPX4 inhibition and ClpP hyperactivation. We also found that ClpP hyperactivation by ONC201 upregulates GPX4 protein expression (**Fig. 5J**). These findings are consistent with a previous study demonstrating upregulation of GPX4 by ETC inhibition [40], suggesting that GPX4 exerts a cell-protective response against mitochondrial proteotoxic stress in AML cells. ClpP hyperactivation sensitized ETC-intact RhoWT cells to GPX4 inhibition, but the synergism was not exerted in Rho0 cells (**Fig. 5K**). This indicates that the induced synergism depends on ETC, which also supports the notion that the regulated protein expression of ETC subunits helps protect cells from ferroptosis.

Discussion

The role of mitochondria in ferroptosis remains controversial partly because of the context-dependent nature of ferroptosis [41, 42]. The findings of the present study demonstrate that intact ETC complexes regulate GPX4 inhibition-mediated ferroptosis in AML cells in a manner distinct from that of other tumor types. Specifically, compared with their parental cells, HL-60-Rho0 cells with ETC defects were more sensitive to GPX4 inhibition. This is in clear contrast with previous studies demonstrating similar or impaired efficacy of the classical GPX4 inhibitor RSL3 against 143B-Rho0 osteosarcoma cells [6] or SK-Hep1 liver sinusoidal endothelial cells [43], respectively. Similarly, another study reported that, in HT-1080 fibrosarcoma cells, mitophagy-mediated mitochondrial depletion blocked erastin-induced ferroptosis while had no effect on RSL3-induced ferroptosis [44]. In the meanwhile, recent CRISPR knockout screening of K562 leukemia cells revealed synthetic lethal interactions between *GPX4* deletion and ETC inhibition [40], which is compatible with our findings. Taken together, our findings suggest that leukemia cells may be distinctively dependent on ETC to protect themselves from ferroptosis.

This mechanism of ETC-dependent protection from ferroptosis could be a therapeutic vulnerability in AML in which GPX4 has been inhibited. Indeed, we observed that the combination of GPX4 inhibition and ClpP activation-mediated degradation of ETC proteins had synergistic anti-leukemia effects in AML

cells. We acknowledge that ClpP targets not only ETC proteins but also other proteins, including those involved in mitochondrial translation or metabolic pathways [37], and the inhibition of such proteins could contribute to the cells' increased vulnerability to GPX4 inhibition-mediated ferroptosis. As another potential mechanism underlining the observed combinatorial effects, we had previously reported that ClpP hyperactivation induces atypical integrated stress response (ISR) and ATF4 upregulation [37, 45]. A recent study shows that ISR-mediated ATF4 activation sensitizes cells to GPX4 inhibition through alteration of GSH metabolism [46]. Involvement of these pathways should also be evaluated in future studies. Nevertheless, the combinatorial effects of ClpP hyperactivation and GPX4 inhibition observed in parental AML cells but not in ETC-deficient Rho0 cells strongly suggest that this synergism and the ferroptosis protection mechanism both depend on intact ETC complexes.

Furthermore, we demonstrated that MitoQ had unexpectedly potent anti-ferroptotic effects in AML cells but, as reported previously, not in MEFs. The importance of mitochondria-localized CoQ is also in line with ETCs' protective effects against mitochondrial lipid peroxidation and resultant ferroptosis because ETCs, particularly complexes I and II, reduce mitochondria-localized CoQ to CoQH₂, which exerts anti-oxidative effects [47]. MitoQ has been reported to have similar protective effects in erastin- or RSL3-treated SK-Hep1 liver sinusoidal endothelial cells, in which induced ferroptosis was also associated with mitochondrial lipid peroxidation [43]. In addition, recent studies by Boyi Gan's group demonstrated that DHODH and GPD2 on the mitochondrial membrane, both regulate the recycling of mitochondria-localized CoQ in collaboration with ETC, protect against ferroptosis [10, 11]. Although the functional relevance of these non-ETC enzymes in AML cell ferroptosis remains to be investigated, we speculate that the maintenance of a reduced form of mitochondrial CoQ primarily contributes to ETC's protective role against ferroptosis in AML cells.

Lastly, here we have reported significant *in vivo* anti-leukemia activity of GPX4 inhibition using a genetic approach. At present, none of the publicly available GPX4 inhibitors are fully developed for use in *in vivo* studies due to their suboptimal bioavailability in animal models. The development of specific GPX4 inhibitors with superior pharmacokinetic and pharmacodynamic profiles *in vivo* is warranted for the clinical implementation of GPX4-targeted therapies. In parallel, potential toxicity of GPX4 inhibitors must be evaluated carefully. For example, while multiple genetic models support the tolerability of conditional *GPX4* deletion in normal hematopoiesis [48, 49] and hematopoietic stem cells [50], sensitivity of human normal hematopoietic stem cells to ferroptosis was recently reported [51]. *GPX4* has also been reported to be essential for early embryonic development in mice [52, 53], thus systemic inhibition of GPX4 could affect other organs. Therefore, it would be critical to identify a therapeutic window for GPX4 inhibitors. Development of a combinatorial strategy that would allow to minimize the dose could be another solution, particularly by targeting cancer-specific molecular mechanisms. Multiple lines of evidence suggest that AML cells, especially therapy-resistant AML, depend on mitochondrial respiration and metabolism [54-57]. Consistently, our present study demonstrates that targeting the mitochondrial regulation of ferroptosis could potentiate the therapeutic efficacy of GPX4 inhibition. These data add substantial support to the development of disease-specific ferroptosis-based therapies in AML.

Materials and Methods

Detailed materials and methods can be found in the Supplementary information.

Cell lines and cell culture

Parental AML cells as well as HEK293T cells and MEFs were obtained and cultured as described in Supplemental information. OCI-AML3-CLPP-Y118A cells were established by us and described previously [37]. CRISPR-engineered isogenic MOLM-13 cells with WT *TP53*, *TP53* knock out (KO), or *TP53 R175H* or *R248Q* mutants were provided by Steffen Boettcher (University of Zurich, Zurich, Switzerland) [58]. HL-60-Rho0 and -RhoWT cells were provided by Peng Huang (Department of Molecular Pathology, MD Anderson Cancer Center) [35].

Primary samples

The mononuclear cells were purified from peripheral blood of AML patients and bone marrow of healthy hematopoietic stem cell donors by Ficoll density–gradient centrifugation and were cultured in RPMI 1640 culture media (#MT10040CV, Corning, Corning, NY) supplemented with 100 ng/ml human Flt3-ligand (#300-19, Peprotech, Cranbury, NJ), 100 ng/ml human SCF (#300-07, Peprotech), 20 ng/ml human TPO (#300-18, Peprotech), and 20 ng/ml human IL-3 (#200-03, Peprotech), as well as 100 U/ml penicillin, 100 µg/ml streptomycin, 2 mM L-glutamine, and 10% heat-inactivated fetal bovine serum.

Immunoblot analyses

For the immunoblot analyses, we used anti-GPX4 antibody (#ab125066, Abcam, Cambridge, UK), anti-α-tubulin antibody (#2125; Cell Signaling, Danvers, MA), anti-β-actin antibody (#A5316, MilliporeSigma, Darmstadt, Germany, or #4970, Cell Signaling), anti-EEFSEC antibody (#HPA035795, MilliporeSigma), total oxidative phosphorylation rodent antibody cocktail (#ab110413, Abcam), and anti-ClpP antibody (#HPA010649, MilliporeSigma).

Declarations

Acknowledgements

The authors thank Kenneth Dunner Jr., (MD Anderson Cancer Center High Resolution Electron Microscopy Facility) for assisting with transmission electron microscopy experiments, Steffen Boettcher (University of Zurich, Zurich, Switzerland) for providing cell lines, Joseph A Munch (MD Anderson Cancer Center Science Medical Library) for editing the manuscript, and Boyi Gan (MD Anderson Cancer Center Department of Experimental Radiation Oncology) for reviewing the manuscript.

This work was supported in part by Relay For Life My Oncology Dream Award (Japan Cancer Society) (HA), The Mochida Memorial Foundation for Medical and Pharmaceutical Research (HA), The Research Fellowship (The Uehara Memorial Foundation) (HA), MD Anderson Cancer Center Institutional Research

Grant (JI), New Investigator Research Grant Program (Leukemia Research Foundation) (JI), Leukemia SPORE Development Research Program (NIH) (JI), and Paul & Mary Haas Chair in Genetics (MA). Part of the study was performed in the Flow Cytometry & Cellular Imaging Core Facility and High Resolution Electron Microscopy Facility at MD Anderson Cancer Center, which is supported in part by NCI Cancer Center Support Grant P30CA16672.

Imipridones ONC201 and ONC212 were kindly provided from Chimerix (Durham, NC).

Competing Interests

MA is a stockholder of Chimerix. We have filed invention disclosure forms related to the use of imipridones in cancers.

Author Contributions

HA, MA, and JI designed and conceptualized the study. HA and JI designed experiments. HA, RZ, NB, SJY, and MP performed *in vitro* experiments and analyzed data. HA, RZ, LBO, and SJY performed *in vivo* experiments and analyzed data. YN, PYM, and VRR provided technical and material supports of experiments. ZL and EA performed statistical analyses. HA and JI wrote the manuscript. JI, BZC, MA reviewed/revised the manuscript. All authors read and approved the final paper.

Ethics Approval and Consent to Participate

The mouse studies were performed following the guidelines approved by the Institutional Animal Care and Use Committees at MD Anderson Cancer Center. Primary samples were obtained from AML patients and hematopoietic stem cell donors after acquiring written informed consent following MD Anderson Cancer Center Institutional Review Board protocol and in accordance with the Declaration of Helsinki.

Data Availability

All data generated during this study are included in this published article and its supplementary files. Additional data are available from the corresponding author upon reasonable request.

References

1. National Cancer Institute. Surveillance, Epidemiology, and End Results Program: Cancer Stat Facts: Leukemia — Acute Myeloid Leukemia (AML) 2022 [Available from: <https://seer.cancer.gov/statfacts/html/amyl.html>.
2. Ganzel C, Sun Z, Cripe LD, Fernandez HF, Douer D, Rowe JM, et al. Very poor long-term survival in past and more recent studies for relapsed AML patients: The ECOG-ACRIN experience. *Am J Hematol*. 2018;93(8):1074-81.
3. Kropp EM, Li Q. Mechanisms of resistance to targeted therapies for relapsed or refractory acute myeloid leukemia. *Exp Hematol*. 2022;111:13-24.

4. Ong F, Kim K, Konopleva MY. Venetoclax resistance: mechanistic insights and future strategies. *Cancer Drug Resist.* 2022;5(2):380-400.
5. Lei G, Zhuang L, Gan B. Targeting ferroptosis as a vulnerability in cancer. *Nat Rev Cancer.* 2022;22(7):381-96.
6. Dixon SJ, Lemberg KM, Lamprecht MR, Skouta R, Zaitsev EM, Gleason CE, et al. Ferroptosis: an iron-dependent form of nonapoptotic cell death. *Cell.* 2012;149(5):1060-72.
7. Yang WS, SriRamaratnam R, Welsch ME, Shimada K, Skouta R, Viswanathan VS, et al. Regulation of ferroptotic cancer cell death by GPX4. *Cell.* 2014;156(1-2):317-31.
8. Bersuker K, Hendricks JM, Li Z, Magtanong L, Ford B, Tang PH, et al. The CoQ oxidoreductase FSP1 acts parallel to GPX4 to inhibit ferroptosis. *Nature.* 2019;575(7784):688-92.
9. Doll S, Freitas FP, Shah R, Aldrovandi M, da Silva MC, Ingold I, et al. FSP1 is a glutathione-independent ferroptosis suppressor. *Nature.* 2019;575(7784):693-8.
10. Mao C, Liu X, Zhang Y, Lei G, Yan Y, Lee H, et al. DHODH-mediated ferroptosis defence is a targetable vulnerability in cancer. *Nature.* 2021;593(7860):586-90.
11. Wu S, Mao C, Kondiparthi L, Poyurovsky MV, Olszewski K, Gan B. A ferroptosis defense mechanism mediated by glycerol-3-phosphate dehydrogenase 2 in mitochondria. *Proc Natl Acad Sci U S A.* 2022;119(26):e2121987119.
12. Kraft VAN, Bezjian CT, Pfeiffer S, Ringelstetter L, Muller C, Zandkarimi F, et al. GTP Cyclohydrolase 1/Tetrahydrobiopterin Counteract Ferroptosis through Lipid Remodeling. *ACS Cent Sci.* 2020;6(1):41-53.
13. Soula M, Weber RA, Zilka O, Alwaseem H, La K, Yen F, et al. Metabolic determinants of cancer cell sensitivity to canonical ferroptosis inducers. *Nat Chem Biol.* 2020;16(12):1351-60.
14. Weitzel F, Ursini F, Wendel A. Phospholipid hydroperoxide glutathione peroxidase in various mouse organs during selenium deficiency and repletion. *Biochim Biophys Acta.* 1990;1036(2):88-94.
15. Hole PS, Darley RL, Tonks A. Do reactive oxygen species play a role in myeloid leukemias? *Blood.* 2011;117(22):5816-26.
16. Lopes M, Duarte TL, Teles MJ, Mosteo L, Chacim S, Aguiar E, et al. Loss of erythroblasts in acute myeloid leukemia causes iron redistribution with clinical implications. *Blood Adv.* 2021;5(16):3102-12.
17. Yu Y, Xie Y, Cao L, Yang L, Yang M, Lotze MT, et al. The ferroptosis inducer erastin enhances sensitivity of acute myeloid leukemia cells to chemotherapeutic agents. *Mol Cell Oncol.* 2015;2(4):e1054549.
18. Ye F, Chai W, Xie M, Yang M, Yu Y, Cao L, et al. HMGB1 regulates erastin-induced ferroptosis via RAS-JNK/p38 signaling in HL-60/NRAS(Q61L) cells. *Am J Cancer Res.* 2019;9(4):730-9.
19. Yusuf RZ, Saez B, Sharda A, van Gastel N, Yu VWC, Baryawno N, et al. Aldehyde dehydrogenase 3a2 protects AML cells from oxidative death and the synthetic lethality of ferroptosis inducers. *Blood.* 2020;136(11):1303-16.

20. Birsen R, Larrue C, Decroocq J, Johnson N, Guiraud N, Gotanegre M, et al. APR-246 induces early cell death by ferroptosis in acute myeloid leukemia. *Haematologica*. 2022;107(2):403-16.
21. Pardieu B, Pasanisi J, Ling F, Dal Bello R, Penneroux J, Su A, et al. Cystine uptake inhibition potentiates front-line therapies in acute myeloid leukemia. *Leukemia*. 2022;36(6):1585-95.
22. Shimada K, Bachman JA, Muhlich JL, Mitchison TJ. shinyDepMap, a tool to identify targetable cancer genes and their functional connections from Cancer Dependency Map data. *Elife*. 2021;10.
23. Zhou N, Bao J. FerrDb: a manually curated resource for regulators and markers of ferroptosis and ferroptosis-disease associations. *Database (Oxford)*. 2020;2020(baaa021).
24. Zhou N, Yuan X, Du Q, Zhang Z, Shi X, Bao J, et al. FerrDb V2: update of the manually curated database of ferroptosis regulators and ferroptosis-disease associations. *Nucleic Acids Res*. 2023;51(D1):D571-D82.
25. Wei J, Xie Q, Liu X, Wan C, Wu W, Fang K, et al. Identification the prognostic value of glutathione peroxidases expression levels in acute myeloid leukemia. *Ann Transl Med*. 2020;8(11):678.
26. Shi ZZ, Tao H, Fan ZW, Song SJ, Bai J. Prognostic and Immunological Role of Key Genes of Ferroptosis in Pan-Cancer. *Front Cell Dev Biol*. 2021;9:748925.
27. Viswanathan VS, Ryan MJ, Dhruv HD, Gill S, Eichhoff OM, Seashore-Ludlow B, et al. Dependency of a therapy-resistant state of cancer cells on a lipid peroxidase pathway. *Nature*. 2017;547(7664):453-7.
28. Eaton JK, Furst L, Ruberto RA, Moosmayer D, Hilpmann A, Ryan MJ, et al. Selective covalent targeting of GPX4 using masked nitrile-oxide electrophiles. *Nat Chem Biol*. 2020;16(5):497-506.
29. Kloditz K, Fadeel B. Three cell deaths and a funeral: macrophage clearance of cells undergoing distinct modes of cell death. *Cell Death Discov*. 2019;5:65.
30. Simonovic M, Puppala AK. On elongation factor eEFSec, its role and mechanism during selenium incorporation into nascent selenoproteins. *Biochim Biophys Acta Gen Subj*. 2018;1862(11):2463-72.
31. Hangauer MJ, Viswanathan VS, Ryan MJ, Bole D, Eaton JK, Matov A, et al. Drug-tolerant persister cancer cells are vulnerable to GPX4 inhibition. *Nature*. 2017;551(7679):247-50.
32. Jiang L, Kon N, Li T, Wang SJ, Su T, Hibshoosh H, et al. Ferroptosis as a p53-mediated activity during tumour suppression. *Nature*. 2015;520(7545):57-62.
33. Sun MG, Williams J, Munoz-Pinedo C, Perkins GA, Brown JM, Ellisman MH, et al. Correlated three-dimensional light and electron microscopy reveals transformation of mitochondria during apoptosis. *Nat Cell Biol*. 2007;9(9):1057-65.
34. Friedmann Angeli JP, Schneider M, Proneth B, Tyurina YY, Tyurin VA, Hammond VJ, et al. Inactivation of the ferroptosis regulator Gpx4 triggers acute renal failure in mice. *Nat Cell Biol*. 2014;16(12):1180-91.
35. Pelicano H, Feng L, Zhou Y, Carew JS, Hileman EO, Plunkett W, et al. Inhibition of mitochondrial respiration: a novel strategy to enhance drug-induced apoptosis in human leukemia cells by a reactive oxygen species-mediated mechanism. *J Biol Chem*. 2003;278(39):37832-9.

36. Guerrero-Castillo S, van Strien J, Brandt U, Arnold S. Ablation of mitochondrial DNA results in widespread remodeling of the mitochondrial complexome. *EMBO J.* 2021;40(21):e108648.
37. Ishizawa J, Zarabi SF, Davis RE, Halgas O, Nii T, Jitkova Y, et al. Mitochondrial ClpP-Mediated Proteolysis Induces Selective Cancer Cell Lethality. *Cancer Cell.* 2019;35(5):721-37 e9.
38. Jacques S, van der Sloot AM, C CH, Coulombe-Huntington J, Tsao S, Tollis S, et al. Imipridone Anticancer Compounds Ectopically Activate the ClpP Protease and Represent a New Scaffold for Antibiotic Development. *Genetics.* 2020;214(4):1103-20.
39. Conrad M, Proneth B. Selenium: Tracing Another Essential Element of Ferroptotic Cell Death. *Cell Chem Biol.* 2020;27(4):409-19.
40. To TL, Cuadros AM, Shah H, Hung WHW, Li Y, Kim SH, et al. A Compendium of Genetic Modifiers of Mitochondrial Dysfunction Reveals Intra-organelle Buffering. *Cell.* 2019;179(5):1222-38 e17.
41. Magtanong L, Mueller GD, Williams KJ, Billmann M, Chan K, Armenta DA, et al. Context-dependent regulation of ferroptosis sensitivity. *Cell Chem Biol.* 2022.
42. Gan B. Mitochondrial regulation of ferroptosis. *J Cell Biol.* 2021;220(9).
43. Oh SJ, Ikeda M, Ide T, Hur KY, Lee MS. Mitochondrial event as an ultimate step in ferroptosis. *Cell Death Discov.* 2022;8(1):414.
44. Gao M, Yi J, Zhu J, Minikes AM, Monian P, Thompson CB, et al. Role of Mitochondria in Ferroptosis. *Mol Cell.* 2019;73(2):354-63 e3.
45. Ishizawa J, Kojima K, Chachad D, Ruvolo P, Ruvolo V, Jacamo RO, et al. ATF4 induction through an atypical integrated stress response to ONC201 triggers p53-independent apoptosis in hematological malignancies. *Sci Signal.* 2016;9(415):ra17.
46. Chen MS, Wang SF, Hsu CY, Yin PH, Yeh TS, Lee HC, et al. CHAC1 degradation of glutathione enhances cystine-starvation-induced necroptosis and ferroptosis in human triple negative breast cancer cells via the GCN2-eIF2alpha-ATF4 pathway. *Oncotarget.* 2017;8(70):114588-602.
47. Wang Y, Hekimi S. Understanding Ubiquinone. *Trends Cell Biol.* 2016;26(5):367-78.
48. Canli O, Alankus YB, Grootjans S, Vegi N, Hultner L, Hoppe PS, et al. Glutathione peroxidase 4 prevents necroptosis in mouse erythroid precursors. *Blood.* 2016;127(1):139-48.
49. Altamura S, Vegi NM, Hoppe PS, Schroeder T, Aichler M, Walch A, et al. Glutathione peroxidase 4 and vitamin E control reticulocyte maturation, stress erythropoiesis and iron homeostasis. *Haematologica.* 2020;105(4):937-50.
50. Hu Q, Zhang Y, Lou H, Ou Z, Liu J, Duan W, et al. GPX4 and vitamin E cooperatively protect hematopoietic stem and progenitor cells from lipid peroxidation and ferroptosis. *Cell Death Dis.* 2021;12(7):706.
51. Zhao J, Jia Y, Mahmut D, Deik AA, Jeanfavre S, Clish CB, et al. Human hematopoietic stem cell vulnerability to ferroptosis. *Cell.* 2023;186(4):732-47.
52. Imai H, Hirao F, Sakamoto T, Sekine K, Mizukura Y, Saito M, et al. Early embryonic lethality caused by targeted disruption of the mouse PHGPx gene. *Biochem Biophys Res Commun.* 2003;305(2):278-86.

53. Yant LJ, Ran Q, Rao L, Van Remmen H, Shibatani T, Belter JG, et al. The selenoprotein GPX4 is essential for mouse development and protects from radiation and oxidative damage insults. *Free Radic Biol Med*. 2003;34(4):496-502.
54. Skrtic M, Sriskanthadevan S, Jhas B, Gebbia M, Wang X, Wang Z, et al. Inhibition of mitochondrial translation as a therapeutic strategy for human acute myeloid leukemia. *Cancer Cell*. 2011;20(5):674-88.
55. Pan R, Ruvolo V, Mu H, Levenson JD, Nichols G, Reed JC, et al. Synthetic Lethality of Combined Bcl-2 Inhibition and p53 Activation in AML: Mechanisms and Superior Antileukemic Efficacy. *Cancer Cell*. 2017;32(6):748-60 e6.
56. Molina JR, Sun Y, Protopopova M, Gera S, Bandi M, Bristow C, et al. An inhibitor of oxidative phosphorylation exploits cancer vulnerability. *Nat Med*. 2018;24(7):1036-46.
57. Bosc C, Saland E, Bousard A, Gadaud N, Sabatier M, Cognet G, et al. Mitochondrial inhibitors circumvent adaptive resistance to venetoclax and cytarabine combination therapy in acute myeloid leukemia. *Nat Cancer*. 2021;2(11):1204-23.
58. Boettcher S, Miller PG, Sharma R, McConkey M, Leventhal M, Krivtsov AV, et al. A dominant-negative effect drives selection of TP53 missense mutations in myeloid malignancies. *Science*. 2019;365(6453):599-604.
59. Carter BZ, Mak PY, Tao W, Zhang Q, Ruvolo V, Kuruvilla VM, et al. Maximal Activation of Apoptosis Signaling by Cotargeting Antiapoptotic Proteins in BH3 Mimetic-Resistant AML and AML Stem Cells. *Mol Cancer Ther*. 2022;21(6):879-89.

Figures

Figure 1.

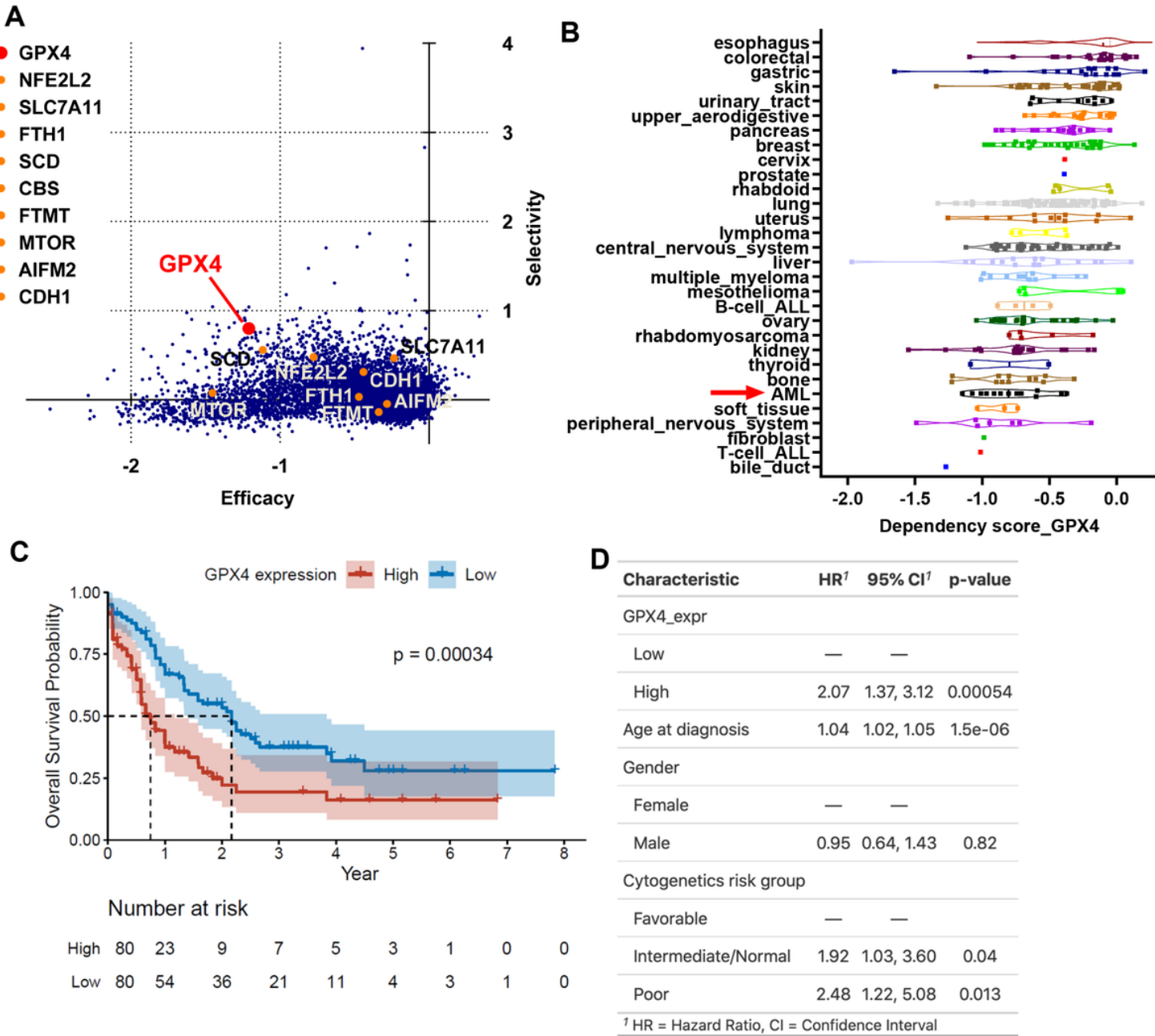


Figure 1

GPX4 has therapeutic potential and prognostic relevance in AML

- A.** Efficacy/selectivity plot for the whole genes analyzed on shinyDepMap. The top 10 ferroptosis suppressor genes on FerrDb are annotated.
- B.** GPX4 dependency scores for all cell lines are clustered by their lineages. A lower dependency score indicates a higher dependency on GPX4. Leukemia cell lines are subdivided into AML, B-cell ALL, and T-cell ALL, based on the original DepMap annotations.

C. Kaplan-Meier plots of the overall survival of AML patients in the TCGA dataset who had high or low GPX4 mRNA expression. The median GPX4 mRNA expression value was used as the cutoff.

D. Results of the multivariate Cox regression model analysis using the TCGA data for GPX4 expression and survival. Age at diagnosis, gender, and cytogenetics risk group are adjusted in the model.

Figure 2.

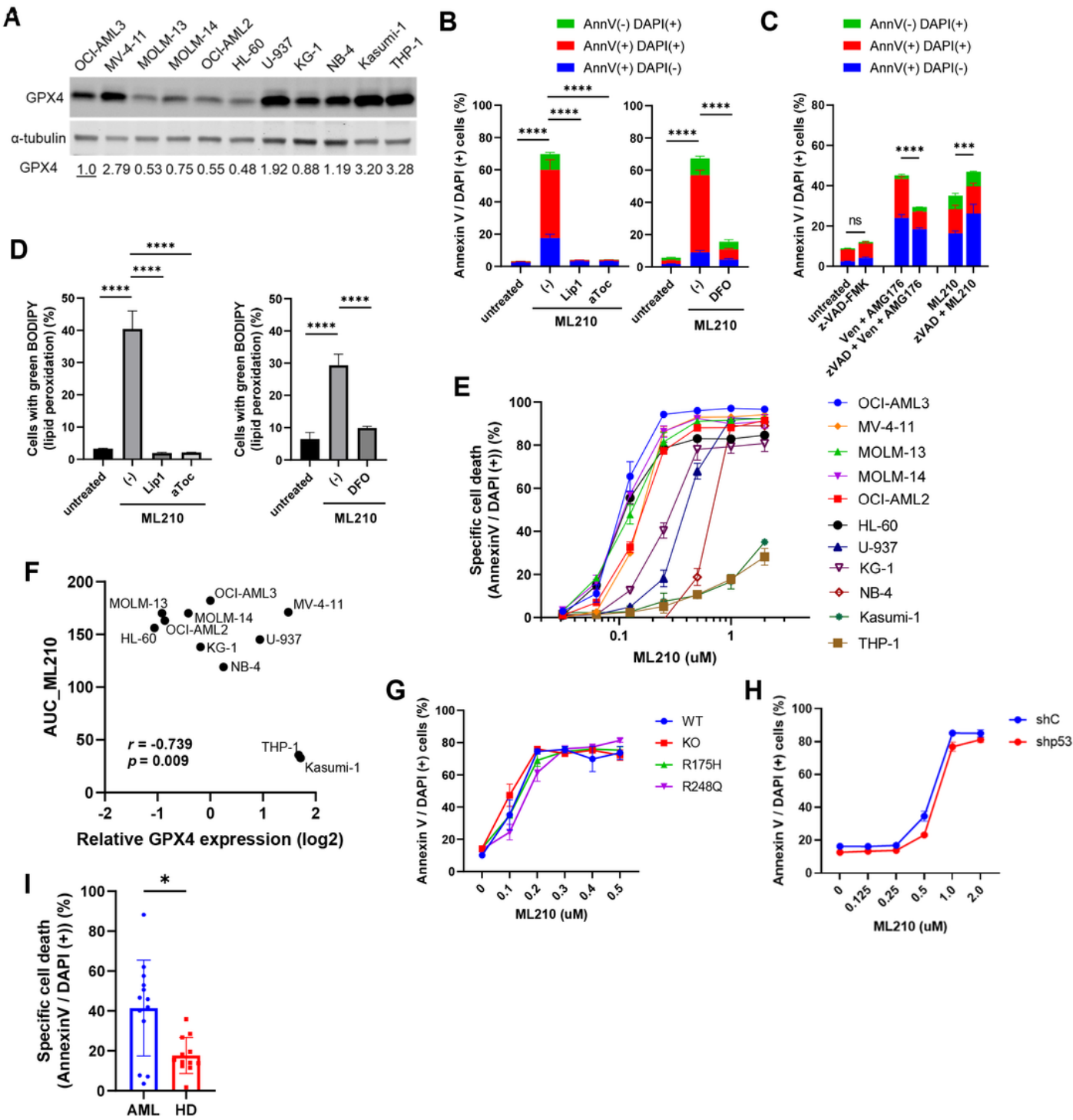


Figure 2

The pharmacological inhibition of GPX4 induces ferroptosis in AML

- A.** GPX4 protein levels in 11 AML cell lines were determined by Western blotting. The relative expression levels of GPX4 were assessed with densitometry as a ratio of GPX4 to α -tubulin (the loading control) and normalized against that of OCI-AML3.
- B, D.** OCI-AML3 cells were treated with 0.5 μ M ML210 with or without 1 μ M liproxstatin-1 (Lip1), 100 μ M α -tocopherol (aToc), or 4 μ M deferoxamine (DFO) for 48 hours. Cell death (B) and lipid peroxidation (D) were determined by annexin V (AnnV) and/or DAPI positivity or by C11-BODIPY581/591 staining, respectively, on flow cytometry.
- C.** OCI-AML3 cells were treated with 1 μ M venetoclax (Ven) plus 0.2 μ M AMG-176 (MCL-1 inhibitor) to induce apoptosis [59] or 0.2 μ M ML210, with or without 25 μ M z-VAD-FMK (zVAD), for 24 hours.
- E.** Parental AML cells were treated with ML210 for 24 hours, and specific cell death was calculated.
- F.** For each cell line, the area under the cell killing curve (AUC) for ML210 (Fig. 2E) was correlated with the relative GPX4 expression level (Fig. 2A). Correlation coefficient (r) and statistical significance (p) on Pearson correlation analysis were indicated.
- G.** CRISPR-engineered MOLM-13 cells with wildtype *TP53* (WT), *TP53* knockout (KO), or the indicated *TP53* mutations were treated with ML210 for 72 hours.
- H.** Kasumi-1 cells transfected with shRNA targeting *TP53* (shp53) or with scramble control shRNA (shC) were treated with ML210 for 72 hours.
- I.** Primary cells from AML patients or healthy bone marrow donors (HD) were treated with 10 μ M ML210 for 48 hours. Cell death was determined for CD45+ cell populations.

A OCI AML3-
shC shGPX4-1 shGPX4-2
Dox - + - + - +
GPX4
β-actin
GPX4 1.0 0.86 1.0 0.11 1.0 0.08

B
Annexin V / DAPI (+) cells (%)
Cells with green BODIPY (lipid peroxidation) (%)
shC shGPX4-1
96h

C OCI-AML3
Annexin V / DAPI (+) cells (%)
shC shGPX4-1 shGPX4-2
Dox (ng/ml)

D MOLM-13
Annexin V / DAPI (+) cells (%)
shC shGPX4-1 shGPX4-2
Dox (ng/ml)

E OCI-AML2
Annexin V / DAPI (+) cells (%)
shC shGPX4-1 shGPX4-2
Dox (ng/ml)

F
Annexin V / DAPI (+) cells (%)
Untreated Dox ML210 Dox + ML210
shC shGPX4-1 shGPX4-2

G
Tetracycline
Survival (%)
Vehicle Tetracycline
Median survival
Vehicle; 55 days
Tetracycline; 74 days
 $p = 0.0048$ (Long rank test)
Engraftment
Days from injection

The genetic knockdown of *GPX4* induces ferroptosis in AML *in vitro* and *in vivo*

B. OCI-AML3-shGPX4-1 cells were treated for with 1 $\mu\text{g}/\text{ml}$ Dox for 96 hours, and cell death and lipid peroxidation were determined by flow cytometry.

Page 19/23

F. OCI-AML3-shGPX4 cells were treated with 0.1 $\mu\text{g/ml}$ Dox for 72 hours in combination with 0.1 μM ML210 for the last 24 hours.

G. Survival curves of the NSG mice transplanted with luciferase-labeled OCI-AML3-shGPX4 cells and treated with vehicle or tetracycline water (n = 7 for each group).

Figure 4.

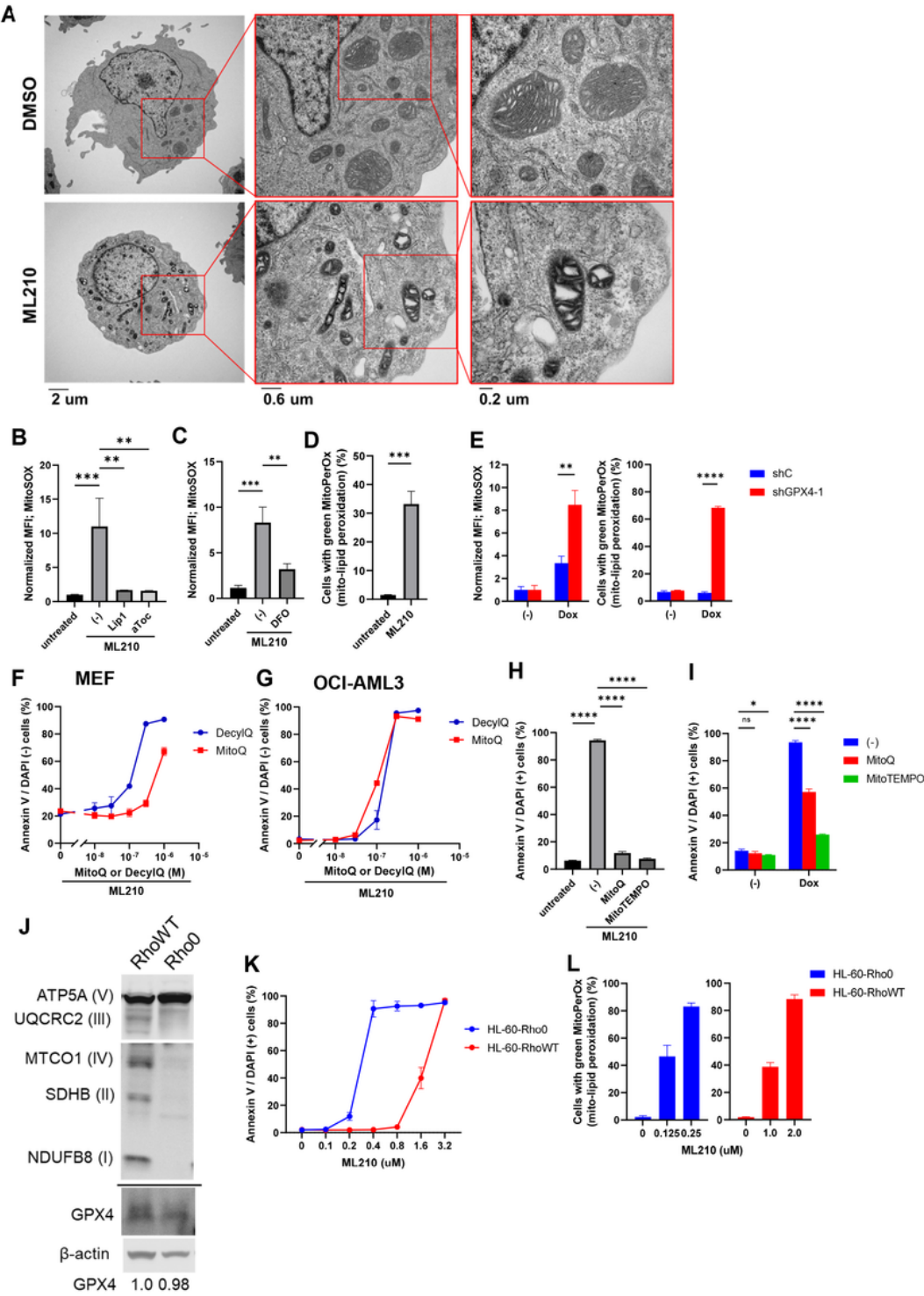


Figure 4

Mitochondrial lipid peroxidation and electron transport chain complexes regulate AML cell ferroptosis

- A.** OCI-AML3 cells were treated with 0.5 μ M ML210 or with DMSO as a control for 6 hours and then subjected to transmission electron microscopy to assess the mitochondrial ultrastructure.
- B, C.** OCI-AML3 cells were treated with 0.5 μ M ML210 with or without 1 μ M liproxstatin-1 (Lip1) (B), 100 μ M α -tocopherol (aToc) (B), or 4 μ M deferoxamine (DFO) (C) for 48 hours. Mitochondrial superoxide production was determined by MitoSOX staining and flow cytometry. The median fluorescence intensity (MFI) of the treated cells was normalized against that of the untreated cells.
- D.** OCI-AML3 cells were treated with 0.4 μ M ML210 for 24 hours, and mitochondrial lipid peroxidation was determined by MitoPerOx staining and flow cytometry.
- E.** OCI-AML3-shGPX4 cells were treated with 1 μ g/ml doxycycline (Dox) for 96 hours.
- F, G.** MEFs (F) or OCI-AML3 cells (G) were treated with 2.0 μ M ML210 in combination with increasing concentrations of MitoQ or DecylQ for 24 hours. Cell viability was determined as the percentage of annexin V⁻ and DAPI-negative cells on flow cytometry.
- H.** OCI-AML3 cells were treated with 0.3 μ M ML210 with or without 0.1 μ M MitoQ or 10 μ M MitoTEMPO for 72 hours.
- I.** OCI-AML3-shGPX4-1 cells were treated with 1 μ g/ml Dox with or without 0.1 μ M MitoQ or 10 μ M MitoTEMPO for 120 hours.
- J.** Lysates from HL-60-RhoWT cells or -Rho0 cells were subjected to Western blotting for the indicated proteins. β -actin was used as a loading control.
- K, L.** HL-60-Rho0 cells or -RhoWT cells were treated with ML210 for 48 (K) or 24 (L) hours.

Figure 5.

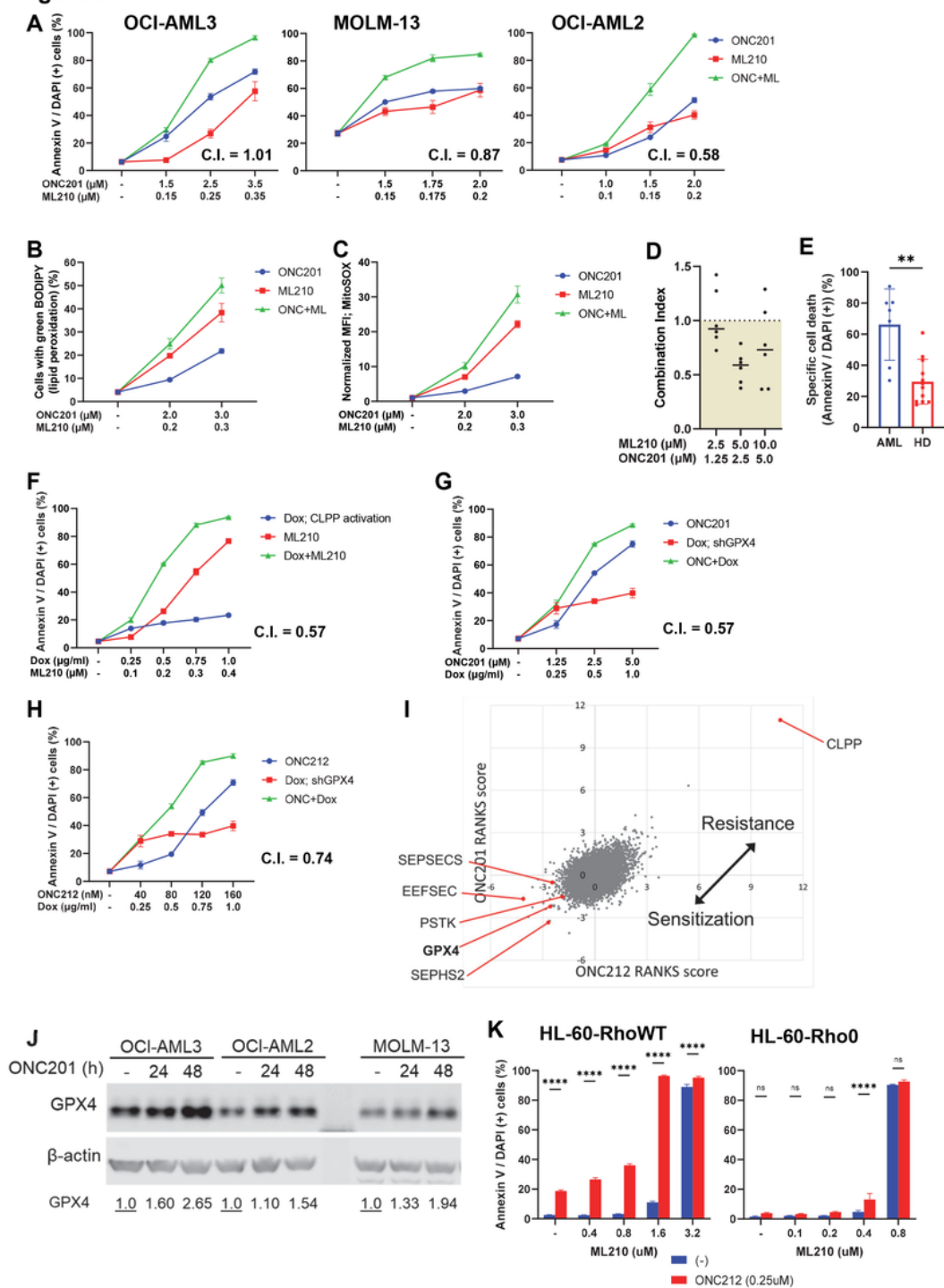


Figure 5

K. HL-60-RhoWT cells or -Rho0 cells were treated with ML210 with or without 0.25 μ M ONC212 for 48 hours.

GPX4 inhibition-mediated ferroptosis is synergistically enhanced by ClpP hyperactivation

- A.** OCI-AML3, MOLM-13, and OCI-AML2 cells were treated with ONC201 and/or ML210 for 72 hours, and cell death was determined by flow cytometry. A combination index (C.I.) less than 1.0 indicates synergistic effects.
- B, C.** OCI-AML3 cells were treated with ONC201 and/or ML210 for 48 hours, and lipid peroxidation (B) and mitochondrial superoxide production (C) were determined by flow cytometry.
- D.** Primary cells from AML patients were treated with ML210 and/or ONC201 for 48 hours. Combination indexes were calculated based on specific cell death in CD45⁺ population for each sample and were plotted.
- E.** Primary cells from AML patients or healthy bone marrow donors (HD) were treated with 10 μ M ML210 and 5 μ M ONC201 for 48 hours, and cell death was determined for CD45⁺ populations.
- F.** OCI-AML3-CLPP-Y118A cells were treated with doxycycline (Dox) for 144 hours in combination with ML210 for the last 72 hours.
- G, H.** OCI-AML3-shGPX4-1 cells were treated with Dox for 120 hours in combination with ONC201 (G) or ONC212 (H) for the last 72 hours.
- I.** A genome-wide CRISPR knockout screening performed on NALM6 cells treated with ClpP agonists were re-analyzed and sgRNA frequency scores (RANKS scores) were plotted.
- J.** OCI-AML3, OCI-AML2, and MOLM-13 cells were treated with 2 μ M ONC201 for up to 48 hours, and GPX4 expression was determined by Western blotting.

Supplementary Files

This is a list of supplementary files associated with this preprint. Click to download.

- [FiguresSupplementaryFinal03072023FigureS1.pdf](#)
- [FiguresSupplementaryFinal03072023FigureS2.pdf](#)
- [FiguresSupplementaryFinal03072023FigureS3.pdf](#)
- [FiguresSupplementaryFinal03072023FigureS4.pdf](#)
- [FiguresSupplementaryFinal03072023FigureS5.pdf](#)
- [SupplementalinformationwithoutFigsfinal03072023.docx](#)
- [SupplementaryTableS1final03012023.pdf](#)
- [Graphicalabstract03012023.docx](#)